

THE Au₃Pd(001) SURFACE STUDIED BY ION SCATTERING AND LEED

S. SPELLER, M. ASCHOFF, J. KUNTZE and W. HEILAND
Universität Osnabrück, 49069 Osnabrück, Germany

A. ATREI
*Dipartimento di Scienze e Tecnologie Chimiche e dei Biosistemi,
Università di Siena, 53100 Siena, Italy*

U. BARDI
Dipartimento di Chimica, Università di Firenze, 50121 Firenze, Italy

E. PLATZGUMMER
Inst. für Allgemeine Physik, TU Wien, A-1040 Wien, Austria

Received 12 September 1999

The (001) surface of a Au₃Pd single crystal was studied with different surface analytical techniques. The main results reported about structure, composition and dynamics of the surface are based on ion scattering methods and LEED. We find segregation of Au to the surface forming a complete Au overlayer. The second layer has approximately the bulk Pd concentration. There is no evidence for chemical order in the near surface layers, i.e. Pd is randomly distributed in the lattice. The Au and Pd atoms in the first and the second layer respectively have approximately the same thermal vibrational amplitudes.

1. Introduction

The Au₃Pd single crystal surfaces have not been studied in great detail so far. The Au₃Pd(110) surface¹ shows segregation of Au to the top layers and the (1 × 2) missing row reconstruction known from the clean Au(110) surface. The Au₃Pd(001)^{2,3} and the Au₃Pd(113)⁴ show full segregation, too, i.e. in the outermost layer only Au atoms are present, and no reconstruction. None of the different crystals studied showed chemical bulk order in X-ray diffraction (XRD). The Pd atoms occupy Au lattice sites randomly within the analytical range of low energy electron diffraction (LEED) (four layers) and neutral impact collision ion scattering spectrometry (NICISS)⁵ (two layers). The Au₃Pd(001) has the singular property, not observed for other systems, that the Au(001) top layer has a smaller lattice constant than bulk Au and bulk Au₃Pd, respectively.² Furthermore, this Au(001) overlayer is not reconstructed

compared to the Au(001) surface on Au. These data on Au₃Pd(001) were obtained by scanning tunneling microscopy (STM), LEED, ion scattering spectrometry and X-ray analysis.^{2,3} Here we report in some detail the NICISS analysis of the Au₃Pd(001) surface with respect to the structure, the composition and the surface thermal vibrations in comparison with the LEED analysis in parts published previously.^{2,3}

2. Experiment

For the ion scattering experiments we use an ultrahigh vacuum (UHV) system equipped with an ion source, mass separating magnet, target chamber with a three-axis target manipulator and several ion detectors. The primary beam can be chopped in order to perform time-of-flight (TOF) analysis of the scattered particles. The advantage of the TOF analysis is low primary ion beam currents due to the detectability of neutrals.⁵ For the experiments

presented here we use a TOF detector placed at a scattering angle of $\Theta = 165^\circ$. Using this detector two modes of ion scattering are feasible: (i) the surface blocking mode, in which the (grazing) angle of incidence ψ is kept constant at around $\psi = 10^\circ$ and the azimuthal angle ϕ is varied; and (ii) the NICISS mode, in which the azimuthal angle ϕ is fixed such the plane of scattering coincides with a low index surface crystallographic surface direction and the angle of incidence is varied. The surface blocking mode gives intensity I vs the azimuthal angle ϕ data which represent a real space projection of the surface structure. From the I vs ϕ data the orientation of the crystal is obtained, i.e. low index directions can be identified. These directions are marked by minima. The depth of the minima is a qualitative measure of the order of the surface, i.e. steps cause an increase of the intensity at the position of the minima in the I vs ϕ curves. For the same purposes, orientation and check of the surface quality, we use LEED as well. For probing the surface chemical composition we use low energy ion scattering (LEIS) with an electrostatic analyzer (ESA).⁵

The Tensor (T) LEED analysis³ is based on $I(V)$ curves measured in different UHV systems in Firenze and in Vienna. In all UHV systems, in Osnabrück, Firenze and Vienna, we used identical preparations. The $\text{Au}_3\text{Pd}(001)$ is sputtered with low energy (500 eV) Ar ions and intermittently annealed at 775 K. The annealing temperature is kept below the order-disorder transition temperature of 1123 K of bulk Au_3Pd .⁶ The order-disorder phase transition is disputable because the chemical ordering has been reported only once⁷ and could not be reproduced.⁸ So Au_3Pd is considered as a solid solution. In Firenze the surface composition is probed by LEIS and XPS, in Vienna by STM and ISS. For further details see Ref. 3.

The Au_3Pd crystals were obtained from MATECK, Jülich.

3. Results

The clean and well-annealed $\text{Au}_3\text{Pd}(001)$ surface yields I vs ϕ data with well-defined minima for the $[100]$ and $[1\bar{1}0]$ surface crystallographic directions (Fig. 1). The small intensity maximum in the $[1\bar{1}0]$ minima is due to flux peaking.⁵ The NICISS data of this direction yield the information about the surface lattice constant.² It turns out that the surface

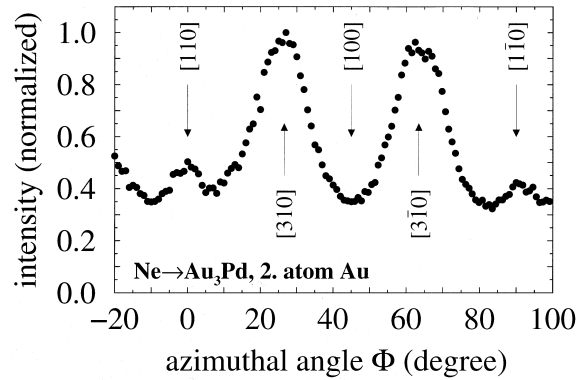


Fig. 1. Backscattered Ne yield of $\text{Au}_3\text{Pd}(001)$ at a grazing angle of incidence of $\Psi = 17.5^\circ$ and a scattering angle of $\Theta = 165^\circ$ as a function of the azimuthal angle (blocking mode). The primary beam energy is 2080 eV.

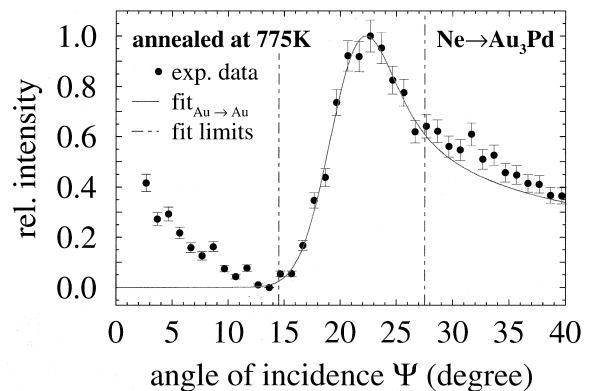


Fig. 2. Backscattered Ne Yield of $\text{Au}_3\text{Pd}(001)$ along the $[100]$ direction (fixed azimuthal angle) at a scattering angle $\Theta = 165^\circ$ as a function of the angle of incidence (NICISS mode). The primary beam energy is 2080 eV. Dots are experimental data; the line is calculated using the two-atom scattering model. The crystal is annealed for 10 min at 775 K.

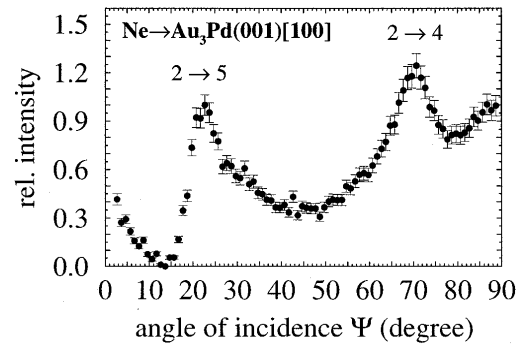
lattice constant $a_s = 3.99 \pm 0.02 \text{ \AA}$ is shortened compared to the bulk lattice constant. The bulk lattice constant is $a_b = 4.017 \pm 0.001 \text{ \AA}$. The surface is not reconstructed, which is confirmed by the TLEED analysis. For the TLEED analysis we use the Barbieri/van Hove code.⁹

The NICISS data of the $[1\bar{1}0]$ direction is shown in Fig. 2. The experimental data are dots with error bars. The line is calculated on the basis of a two-atom scattering mode using a ZBL potential (Ziegler-Biersack-Littmark).⁵ As result of the fit we obtain the lattice constant, the amplitude of the

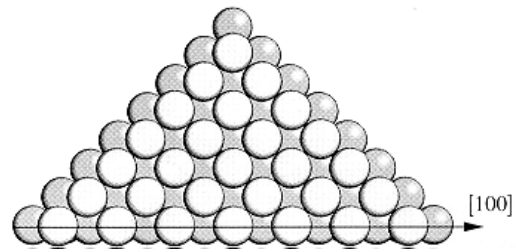
thermal vibrations of the surface atoms within the limits of the Debye model and some information about the relative concentration of Au and Pd. In the case of the well-annealed layer only Au is present in the top layer. The intensity increase at the lowest angles of incidence ψ is due to scattering from steps and from the front edge of the crystal eventually.

The vibrational amplitudes obtained from the NICISS data correspond to Debye temperatures of $\Theta_D = 136 \pm 6$ K for Au atoms and the $[100]$ direction and $\Theta_D = 166 \pm 16$ K for Au atoms and the $[1\bar{1}0]$ direction and $\Theta_D = 219 \pm 5$ K for Pd, respectively. When scattering along $[1\bar{1}0]$ Pd atoms of the second layer are exposed to the ion beam. The main component of the thermal vibrational amplitudes measured is perpendicular to the surface. The magnitude of the amplitudes of Au and Pd are equal. In the TLEED analysis we use the bulk Debye temperatures of Au, $\Theta_D = 165$ K, and of Pd, $\Theta_D = 274$ K, resulting in approximately equal vibrational amplitudes for Au and Pd as in the NICISS evaluation. A variation of Θ_D to the range of the NICISS values does not significantly influence the R factor. Allowing anisotropic vibrations does not improve the R factors significantly. The Pendry R factor (R_P) and the modified Zanazzi–Jona factor (R_{MZJ}) in the TLEED analyses are 0.206 and 0.096, respectively.³

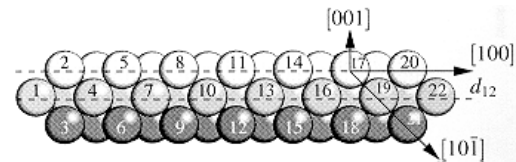
When extending the ψ range in the NICISS experiment, information about the interlayer distance between first and second layer d_{12} becomes available (Fig. 3). The angular difference between the first and the second peak is directly related to d_{12} . The value we obtain is $d_{12} = 1,70 \pm 0.05$ Å, corresponding to a contraction of $15 \pm 3\%$. The TLEED analysis gives $d_{12} = 2.00 \pm 0.03$ Å (Firenze), $d_{12} = 1.99 \pm 0.02$ (Vienna), i.e. no contraction. In Table 1 we



(a)



(b)



(c)

Fig. 3. (a) Experimental data as in Fig. 2 for an extended range of the angle of incidence. The numbers at the peaks identify the two-atom scattering process, i.e. $2 \rightarrow 5$ is surface scattering, as is $5 \rightarrow 8$ etc., and $2 \rightarrow 4$ is first to second layer scattering, as is $5 \rightarrow 7$ etc. The atoms are labeled according to Fig. 3(c). (b) Top view of a model of the $\text{Au}_3\text{Pd}(001)$ surface. White spheres are Au atoms (top layer); gray spheres are Au or Pd atoms of the second layer. (c) Side view of the crystal structure of $\text{Au}_3\text{Pd}(001)$. The numbers are used to identify the scattering peaks of Fig. 3(a).

Table 1. Comparison of crystallographic data and composition evaluated by NICISS and LEED (F = Firenze; W = Vienna). a_s describes the surface lattice constant and d_{12} the spacing between the first and the second layer.

	a_s (Å)	d_{12} (Å)	1st layer Au	2nd layer Au
NICISS	3.99 ± 0.02	1.70 ± 0.05	100%	$60 \pm 30\%$
LEED (F)	4.00 ± 0.01	2.00 ± 0.03	100%	$60 \pm 20\%$
LEED (W)	3.99 ± 0.01	1.99 ± 0.02	100%	$75 \pm 19\%$

Table 2. Surface Debye temperatures of $\text{Au}_3\text{Pd}(001)$ of the $[1\bar{1}0]$ and the $[100]$ directions and of $\text{Au}(100)$ and $\text{Pd}(100)$ surfaces of bulk crystals from theory¹² and experiment.¹³

	$\text{Au}_3\text{Pd}(001)[1\bar{1}0]$	$\text{Au}_3\text{Pd}(001)[100]$	$\text{Au}(001)$	$\text{Pd}(001)$
Au	166 K	136 K	110 K ¹²	–
Pd	219 K		–	189 K, ¹² 156 K ¹³

summarize the data obtained from NICISS and TLEED respectively.

The TLEED analysis yields further data, i.e. the interlayer distances $d_{23} = 1.97 \pm 0.03$ Å (Firenze), $d_{23} = 1.99 \pm 0.02$ (Vienna), $d_{34} = 2.01 \pm 0.03$ Å (Firenze), $d_{34} = 2.00 \pm 0.03$ (Vienna) and the Au concentration of the 3d layer of $60 \pm 20\%$ (Firenze), and $75 \pm 12\%$ (Vienna), which is the bulk value.³

4. Discussion

The $\text{Au}_3\text{Pd}(001)$ surface is fully covered with a monolayer of Au, as are the other surfaces studied, i.e. $\text{Au}_3\text{Pd}(110)$ and $\text{Au}_3\text{Pd}(113)$.^{1,4} The surface related to $\text{Au}_3\text{Pd}(001)$ from the point of view of structure and composition is the $\text{Au}_3\text{Cu}(100)$ surface. The bulk structure of the Cu_3Au alloys is, however, $L1_2$ (Cu_3Au). (Chemical order of Au_3Pd is reported only once,⁷ an observation which could not be reproduced,⁸ whereas the Cu_3Au and Au_3Cu crystals are chemically ordered. Nevertheless the $\text{Au}_3\text{Cu}(100)$ also shows complete segregation of Au, but chemical order in the second layer.¹⁰ In contrast, we have no evidence for chemical order in the analysis of $\text{Au}_3\text{Pd}(100)$ nor of $\text{Au}_3\text{Pd}(110)$ ¹ and $\text{Au}_3\text{Pd}(113)$.⁴ The theoretical modeling of the Au_3Pd crystal¹ gave clear evidence that the crystal is not chemically ordered.

Nevertheless, it is an interesting notion that the $\text{Au}_3\text{Pd}(001)$ surface is covered by a well-ordered $\text{Au}(001)$ monolayer without any signs of reconstruction, whereas the $\text{Au}(001)$ surface of Au is reconstructed.¹¹

In Table 2 we summarize data of Θ_D from different sources, theory and experiment for $\text{Au}_3\text{Pd}(110)$ and for regular $\text{Au}(100)$ and $\text{Pd}(100)$ surfaces, respectively. Only from NICISS do we obtain specific Θ_D values for the respective direction.

The interesting result is that the Au surface Debye temperature is higher than the one calculated for the $\text{Au}(001)$ surface of bulk Au¹² but is equal to the experimental value of $\text{Pd}(001)$.¹³ It may be accidental, but the numbers say that the Au surface atom thermal vibrational amplitudes are dominated by Pd atomic vibrational amplitudes, even though the Pd concentration is minimal in the top surface layer and of the order of 40% or 25% in the second layer. Unfortunately, the TLEED analysis is not significantly dependent on Θ_D in the range of the NICISS Θ_D data, and thus complementary data for Θ_D are not available.

The interplanar distance d_{12} between the top layer and the second layer is not reduced based on the TLEED analysis, but reduced by 15% based on NICISS. Differences between d_{12} values evaluated by LEED and NICISS have been found before (Ref. 14 and references therein). NICISS data yield systematically larger contractions, i.e. smaller d_{12} values, in cases where comparable data exist. Here we have the first case for LEED and NICISS results of the same sample.

The TLEED result, i.e. no contraction, agrees with the finding for the $\text{Pd}(001)$ surface of Pd.¹⁵ Another hint for the dominating role of Pd? These findings, with respect to Θ_D and d_{12} , may support the model,^{2,16} that the (001) surface of Au_3Pd is stabilized by Au–Pd bonds which are energetically more favorable than Au–Au bonds.

Acknowledgments

This work is supported by the Assistentenprogramm an Niedersächsischen Fachhochschulen, the ESF(ALE.NET), and in part by the DFG. E. P. acknowledges financial support by the Austrian Fonds zur Förderung der wissenschaftlichen Forschung. We thank B. Baretzky (MPI Stuttgart) for the XRD analyses.

References

1. J. Kuntze, S. Speller, W. Heiland, P. Deurinck, C. Creemers, A. Atrei and U. Bardi, *Phys. Rev. B* (1999), in print.
2. M. Aschoff, S. Speller, J. Kuntze, W. Heiland, E. Platzgummer, P. Varga and B. Baretzky, *Surf. Sci. Lett.* **415**, L1051 (1998).
3. J. Kuntze, S. Speller, W. Heiland, A. Atrei, G. Rovida and U. Bardi, *Phys. Rev.* **B60**, 1535 (1999).
4. M. Aschoff, G. Piaszenski, S. Speller and W. Heiland, *Surf. Sci.* **402–404**, 770 (1998).
5. H. Niehus, W. Heiland and E. Taglauer, *Surf. Sci. Rep.* **17**, 213 (1993).
6. O. Madelung (ed.), Landolt-Börnstein new series IV/5a (Springer, Berlin, 1991), p. 402; C. J. Smith, (ed.), Metal Reference Book (Butterworth, London, 1976).
7. A. Nagasawa, Y. Matsuo and J. Kakinoki, *J. Phys. Soc. Jap.* **20**, 1881 (1965).
8. Y. Kawasaki, S. Ino and S. Ogawa, *J. Phys. Soc. Jap.* **30**, 1758 (1971).
9. A. Barbieri and M. A. Van Hove, Symmetrized Automated Tensor LEED package, version 4.1.
10. S. Schömann and E. Taglauer, *Surf. Rev. Lett.* **3**, 1823 (1996).
11. B. M. Ocko, D. Gibbs, K. G. Huang, D. M. Zehner and S. G. J. Mochrie, *Phys. Rev.* **B44**, 6429 (1991); L. Bönig, S. Liu and M. Metiu, *Surf. Sci.* **365**, 87 (1996).
12. D. P. Jackson, *Surf. Sci.* **43**, 431 (1974).
13. C. Waldfried, D. N. McIlroy, J. Zhang, P. A. Dowben, G. A. Katrich and E. W. Plummer, *Surf. Sci.* **363**, 296 (1996).
14. S. Speller, S. Parascandola and W. Heiland, *Surf. Sci.* **383**, 131 (1997).
15. J. M. MacLaren, J. B. Pendry, P. J. Rous, D. K. Salin, G. A. Somorjai, M. A. Van Hove and D. D. Vredensky, *Surface Crystallographic Information Service* (Reidel, 1987).
16. W. Hebenstreit, G. Ritz, M. Schmid, A. Biedermann and P. Varga, *Surf. Sci.* **388**, 150 (1997).